



Photocatalytic-oxidation of solid state chitosan by immobilized bilayer assembly of TiO₂–chitosan under a compact household fluorescent lamp irradiation

M.A. Nawi*, Ali H. Jawad, S. Sabar, W.S. Wan Ngah

School of Chemical Sciences, Universiti Sains Malaysia, 11800 Minden, Penang, Malaysia

ARTICLE INFO

Article history:

Received 20 March 2010

Received in revised form 16 July 2010

Accepted 10 September 2010

Available online 30 October 2010

Keywords:

Chitosan

Oxidation

Photocatalysis

TiO₂

Bilayer system

ABSTRACT

Photocatalytic-oxidation of an immobilized solid state chitosan (CS) by assembling a bilayer TiO₂–CS-glass system in aqueous solution under 45-W compact household fluorescent lamp was investigated. The structural and optical changes of CS were characterized by elemental analysis, Fourier-transform infrared spectroscopy (FT-IR) analysis, UV–vis diffuse reflectance spectroscopy (DRS) analysis and photoluminescence spectroscopy (PLS) analysis. The results indicated the formation of carbonyl side group and elimination of some amino group without altering much of the whole structure of CS. Furthermore, the photocatalytic-oxidation process led to the formation of an irregular surface morphology of CS according to the SEM images. The visual color changed to a more intense brown and less water uptake was also observed. The experimental results show that the bilayer TiO₂–CS-glass arrangement system can be considered as a convenient and environmentally friendly method for green chemistry application, especially in the field of the mild oxidation of a solid state CS.

© 2010 Elsevier Ltd. All rights reserved.

1. Introduction

Chitosan (CS) biopolymer has been effectively degraded from polymeric into oligomeric form by using gamma and e-beam radiation (Gryczka et al., 2009), laser pulses (Kasaai, Arul, Chin, & Charlet, 1999), microwave irradiation (Shao, Yang, & Zhong, 2003), and ultraviolet irradiation (Andrady, Torikai, & Kobatake, 1996). Generally, irradiation of CS basically yields scission of 1–4 glycosidic bonds and the formation of carbonyl side group in the CS oligomer. However, new product from the photo-modified CS without altering much of its polymeric structure is a useful alternative method in the still-developing field of polymer technology. In this regard, only a few reports have been focused on the photo-oxidation of CS without breaking it into oligomers form such as its photo-oxidation under γ -rays (Ulanski & von Sonntag, 2000), or in solid state CS under UV light (Sionkowska, Wisniewski, Skopinska, Vicini, & Marsano, 2005). In fact, in order to fulfill the requirements of obtaining successful photo-modification of CS without significant degradation of its polymeric structure, the presence of oxygen is preferable whereby it is able to reduce considerably the scission of the glycosidic bond (Ulanski & von Sonntag, 2000). In addition, using a solid state form of CS is also preferable in order to prevent

any extensive degradation of the polymer in its water-swollen form (Ulanski & Rosiak, 1992).

Another novel approach to achieve photo-oxidation of CS is via an advanced oxidation process (AOP). In fact, AOPs have been proven to be an effective treatment method for the degradation of toxic organic pollutants from wastewaters. In this application, TiO₂ presents itself to be a bench mark photocatalyst because of its various merits, such as chemical stability, high photocatalytic activity, non-toxicity and excellent ability to degrade numerous kinds of organic pollutant in water to harmless end products of CO₂, H₂O and some simple mineral acids (Gaya & Abdullh, 2008). It is therefore hypothesized that TiO₂ under a mild irradiation process and with a proper assemblage system could oxidize CS in its solid state form without suffering extensive damage to its polymeric backbone. However, to the best of our knowledge, until now, the photocatalytic-oxidation of CS in its solid state form under a low-energy 45-W compact household fluorescent lamp in the presence of TiO₂ has never been reported in the literature. Therefore, this work presents a new photocatalytic-oxidation method of CS in its solid state form which was performed by using a novel assemblage of immobilized bilayer TiO₂–CS-glass system. This immobilized system is a convenient method because the immobilization of TiO₂ can solve the problem of the post-treatment catalyst powder recovery. Additionally, it is an environmental friendly system, since the super oxidizing agents and high-energy light sources are not required and the oxidation process is also applicable at the ambient temperature and pressure.

* Corresponding author. Tel.: +60 4 6534031; fax: +60 4 6574854.
E-mail address: masri@usm.my (M.A. Nawi).

2. Materials and methods

2.1. Materials

CS of medium molecular weight of 322 g mol^{-1} with a 68.20% degree of deacetylation as determined by infrared spectroscopy method (Gryczka et al., 2009) was purchased from Sigma–Aldrich. Titanium (IV) oxide (99% anatase) was obtained from Sigma–Aldrich. Phenol-formaldehyde powder resin (PF) was bought from Borden Chemical Sdn. Bhd, Malaysia. Epoxidized natural rubber (ENR50) was obtained from Kumpulan Guthrie Sdn. Bhd, Malaysia. All the materials were used as received without further purification. Ultra pure water ($18.2 \text{ M}\Omega \text{ cm}^{-1}$) was used in this work.

2.2. Fabricating of an immobilized TiO_2 –CS–glass system

An immobilized bilayer TiO_2 –CS–glass system was fabricated based on our pervious procedure (Nawi, Sabar, Jawad, & Ngah, 2010). Anyhow, CS solution was prepared by adding 6.0 g of CS flakes in 400 mL of 5% (v/v) acetic acid solution and then homogenized by grinding for 30 h using a ball mill grinder. The bubbles-free white viscous CS solution was casted onto glass plates, each of dimension $4.7 \text{ cm} \times 6.5 \text{ cm}$. It was then heated in an oven for 4 h at 100°C in order to remove the solvent. The final form of the immobilized CS on the glass plate (or known as CS-glass) appeared in a light-yellow color. The photocatalyst formulation was prepared by adding fixed amounts of 0.15 g phenol-formaldehyde resin (PF) as a adhesive co-agent and 5 g epoxidized natural rubber (ENR50) solution (11.32% solution of ENR50 in toluene) as a binder to TiO_2 powder into an amber bottle, which contained 12 g TiO_2 powder. Finally, 60 mL of acetone was poured into the bottle before being homogenized by sonication for 5 h. This TiO_2 formulation was used to immobilize TiO_2 onto CS-glass by a simple dip-coating method in order to fabricate a bilayer TiO_2 –CS–glass system.

2.3. Photocatalytic-oxidation of CS

In this study, CS in its solid state form was photocatalytically oxidized by TiO_2 under a low-energy 45-W compact household fluorescent lamp. The photocatalytic oxidation method was based on a novel immobilized bilayer system assembly of TiO_2 –CS–glass whereby CS was made the sub layer while TiO_2 was made the top layer with glass plate used as the support substrate. The thickness of the TiO_2 top layer was determined by SEM microscope to be $40.94 \pm 1.16 \mu\text{m}$ which was obtained by deposition of $1.30 \pm 0.08 \text{ mg cm}^{-2}$ of TiO_2 formulation onto CS-glass, while the thickness of CS sub layer was also determined by SEM microscope to be $6.35 \pm 0.61 \mu\text{m}$ which was obtained by casting $0.65 \pm 0.08 \text{ mg cm}^{-2}$ of CS solution onto a glass plate.

2.4. Measurements

Elemental analysis was carried out by using CHN analyzer (Perkin-Elmer, Series II, 2400). FT-IR spectroscopy of CS was obtained via a Perkin-Elmer FT-IR system, spectrum BX. UV–vis diffuse reflectance spectroscopy (DRS) was via a Perkin-Elmer, Lambda 35 UV–vis spectrometer. Photoluminescence spectrum (PLS) was recorded on Raman and Photoluminescence spectroscopy system (model: Jobin Yvon HR 800 UV). Scanning electron microscopy (SEM-EDX, Model Leica Cambridge S360) was used to observe the surface morphology of CS and also the thickness of the immobilized TiO_2 and CS layers. The leaching ratio (LR) of CS was

calculated according to the following equation:

$$\text{LR (\%)} = \left[\frac{(W_i - W_t)}{W_i} \right] \times 100 \quad (1)$$

where W_i is the initial weight (g) of CS-glass before the photo-oxidation process with 20 mL water while W_t , the remaining weight (g) of CS-glass system after different irradiation time. The swelling index (SI) was followed and calculated exactly based on the procedure described by (Wan, Creber, Peppley, & Bui, 2003), via following formula:

$$\text{SI (\%)} = \left[\frac{(W_w - W_d)}{W_d} \right] \times 100 \quad (2)$$

Where W_d is the weight (g) of dried CS layer while W_w , the weight (g) of wet CS layer. All of the above analyses that include SEM, swelling, PLS, UV–vis DRS, CHN and FT-IR analyses of the CS layer were done by removing the CS layer manually from the glass plate using a razor blade in a very delicate process. While, for the CS sub layer in the bilayer TiO_2 –CS–glass system, the TiO_2 top layer was firstly removed by intensive rinsing with acetone and brushing with a laboratory brush until the entire TiO_2 layer was visually gone. It was then followed by rinsing with ultra pure water and left to dry in air. Finally, the oxidized CS sub layer was carefully removed from the glass plate using a razor blade as described above. The UV leakage of the 45-W fluorescent lamp was determined by using a radiometer (Solar Light Co. PMA 2100) connected with a UV-A and UV-B broadband detector (PMA 2107). This lamp was placed in contact with the outer surface of the ($5 \text{ cm} \times 8 \text{ cm} \times 1 \text{ cm}$) glass photo reactor cell containing 20 mL of ultra pure water. The whole set-up was aerated via a pasteur pipette connected to an aquarium aeration pump. The aeration flow rate was maintained at 25 mL min^{-1} throughout the photocatalytic-oxidation process using a Gilmont direct reading flowmeter. The photo-oxidation process was done by a repeated 2 h radiation exposure with fresh ultra pure water used at every 2 h cycle of irradiation. The process was stopped after a total of 10 h or 5 cycles of irradiation.

3. Results and discussion

3.1. Physical studies

3.1.1. Leaching ratio (LR) measurements

Fig. 1 shows the weight loss of the irradiated CS layer in the CS-glass system and irradiated bilayer TiO_2 –CS–glass system in water in the form of leaching ratio (LR) at different time of irradiation. For controlling purpose, the leaching ratio of irradiated TiO_2 layer in the TiO_2 –glass system and unirradiated bilayer TiO_2 –CS–glass system were taken as references as well. As can be seen, the maximum LR of the irradiated bilayer TiO_2 –CS–glass system was remarkably reduced ($2.43 \pm 0.27\%$) in comparison to the LR of the irradiated CS layer without TiO_2 ($8.36 \pm 0.43\%$). The weight lost of the bilayer TiO_2 –CS–glass system was assumed to be due to the leaching of the CS sub layer as well as the organic additives within the TiO_2 layer. In fact, the LR of the TiO_2 single layer was found to be ($1.52 \pm 0.12\%$) after 10 h of the photocatalytic process. However, the LR of the unirradiated bilayer TiO_2 –CS–glass system did not show any noticeable change after 10 h of placing it in water under the same condition but in the absence of light. This means that the CS sub layer of the bilayer TiO_2 –CS–glass system undergone some transformation during the photocatalytic-oxidation process into a more physically stable form.

3.1.2. Swelling index (SI) measurements

The SI of unirradiated CS layer was measured to be $66.09 \pm 4.86\%$. This relatively high SI was basically due to the existence of the hydrophilic groups, i.e. free hydroxyl and amino groups

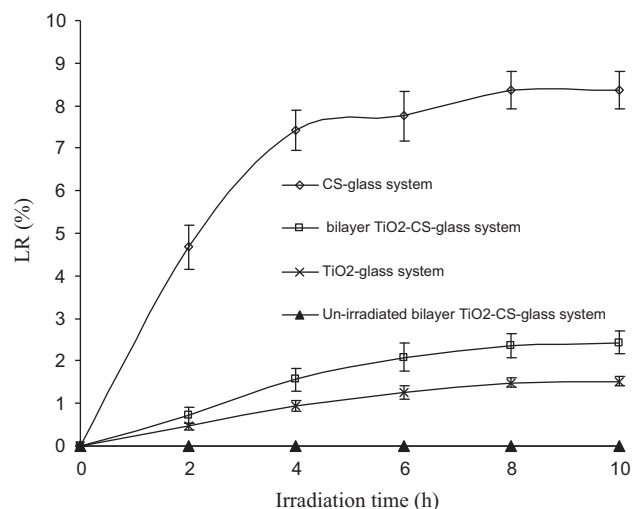


Fig. 1. Measuring the weight loss as a function of the leaching ratio (LR) of the irradiated CS layer in the CS-glass system, irradiated bilayer TiO₂-CS-glass system, irradiated TiO₂ layer in the TiO₂-glass system and unirradiated bilayer TiO₂-CS-glass system at different times of irradiation in water.

in the pyranose ring (Wan et al., 2003). On the other hand, the SI of photocatalytically oxidized CS sub layer in the bilayer TiO₂-CS-glass system was reduced remarkably to $47.53 \pm 5.98\%$ after 10 h of the photocatalytic-oxidation process. This can be attributed to the change in the content of the free amino ($-\text{NH}_2$) and hydroxyl groups of CS during the photocatalytic-oxidation process, and turns the CS structure to be more hydrophobic. This data collaborates well with LR values of CS during photocatalytic-oxidation process. Furthermore, it can be predicted at this stage that the overall polymeric backbone structure of CS remains intact without any degradation, since the photocatalytic-oxidative form of CS exhibits less leachability and swelling capacity. This is contrary to the normally reported results of the degradation process of CS which leads basically to improve its solubility (Liu et al., 2006; Qin et al., 2006).

3.2. Structural studies

3.2.1. Elemental analysis

The CHN compositions of the unirradiated CS layer in the CS-glass system, irradiated CS layer in the CS-glass system and irradiated CS sub layer in the bilayer TiO₂-CS-glass system were taken and the results are listed in Table 1. It was found that the changes in mass ratio of C/H of all systems were minor at the best, while the mass ratio of C/N increased only during the photocatalytic-oxidation process. This observation indicates the possible elimination of partial amino groups during radiation (Huang, Zhai, Peng, Li, & Wei, 2007). It is also important to note the reduction of percent carbon and nitrogen in the photocatalytically oxidized CS as opposed to the unirradiated CS. Therefore not only there was involvement of amino group in the photocatalytic-oxidation process but also a carbon containing group. The overall structure of the CS was expected to be intact, since the mass ratio of C/H did not show any significant difference between the irradiated CS sub layer in the bilayer TiO₂-CS-glass system and the unirradi-

ated CS in the CS-glass system. As for irradiated CS in the CS-glass, a similar assessment can be made whereby it can be concluded that no transformation occurred during the irradiation process.

3.2.2. FT-IR spectral analysis

Fig. 2 shows the FT-IR spectrums of (a) unirradiated CS layer in the CS-glass system, (b) irradiated CS layer in the CS-glass system and (c) irradiated CS sub layer in the bilayer TiO₂-CS-glass system for 10 h in water. As can be seen from spectrum (a), the characteristic bands of CS polysaccharide appeared at around 3432 cm^{-1} (overlapping of the stretching vibration of N-H and O-H functional groups), 1653 cm^{-1} (C=O stretching vibration in amide group, amide I), 1577 cm^{-1} (N-H bending vibration in amide group, amide II), 1419 cm^{-1} (bending vibration of primary amino group, $-\text{NH}_2$), 1380 cm^{-1} (C-N bending vibration) (Ngah & Fatinathan, 2006). The characteristic bands to the saccharied structure were at 1153 cm^{-1} (asymmetrical stretching vibrations of the C-O-C glycosidic bond), 1082 and 1031 cm^{-1} (skeletal vibrations involving the C-O stretching) (Pawlak & Mucha, 2003; Smitha, Sridhar, & Khan, 2005). Meanwhile, bands at 2921, 2875, 1322 and 1261 cm^{-1} are assigned to the asymmetrical and symmetrical stretching vibrations of the CH_2 of pyranose ring (Ostrowska-Czubenko & Gierszewska-Drużyńska, 2009). The evidence obtained from spectrum (b) indicated that there is no obvious modification of chemical structure of CS, except for a slight reduction in the band intensity at around 1577 cm^{-1} which is ascribed to the partial involvement of amino groups in intra- and intermolecular hydrogen bonds (Peter, 2002). However, the result of photocatalytically oxidized CS in spectrum (c) indicated that the amino and hydroxyl characteristic bands of CS generally shifted to lower wavenumbers and new band appears at 1647 cm^{-1} , which is assigned to the elimination of partial amino and hydroxyl groups and the formation of carbonyl (C=O) side groups respectively. In this regard, it was reported that the photo-oxidation of CS caused the formation of carbonyl group which appeared as a new band either at 1640 cm^{-1} (Andrady et al., 1996), or at 1634 cm^{-1} (Shao et al., 2003). Additionally, the rest of the bands in spectrum (c) were almost similar to the bands represented in spectrum (a) and (b). In fact, the distinct band of glycosidic bond does not show noticeable changes neither in the band intensity nor shifting in the wavenumbers as compared to the unirradiated CS (spectrum (a)). This indicates that the photo-oxidation of CS leads to the formation of carbonyl side group without breaking of the glycosidic bond and altering much of the whole chemical structure of CS.

3.3. Optical studies

3.3.1. UV-vis DRS spectral analysis

To further confirm the optical changes of CS during the photocatalytic-oxidation process, UV-vis DRS spectral analysis was carried out on the CS samples. Fig. 3(a) and (b) shows the UV-vis DRS spectrums of unirradiated CS layer in the CS-glass system and irradiated CS sub layer in the bilayer TiO₂-CS-glass system respectively. For spectrum (a), a strong absorption band at around 306 nm is known for natural CS (Andrady et al., 1996). As can be seen in spectrum (b), the new absorption band appears at around 350 nm which can be ascribed to the $n \rightarrow \pi^*$ transition of the newly formed

Table 1
Elements' content of unirradiated CS layer in the CS-glass system, irradiated CS layer without TiO₂ in the CS-glass system and the irradiated CS sub layer with TiO₂ in the bilayer TiO₂-CS-glass system for 10 h in water.

Samples	C%	H%	N%	C/N	C/H
Unirradiated CS layer in the CS-glass system	34.48	6.12	5.85	5.89	5.63
Irradiated CS layer in the CS-glass system	34.39	5.98	5.82	5.90	5.75
Irradiated CS sub layer in the bilayerTiO ₂ -CS-glass system	32.66	5.89	4.63	7.05	5.54

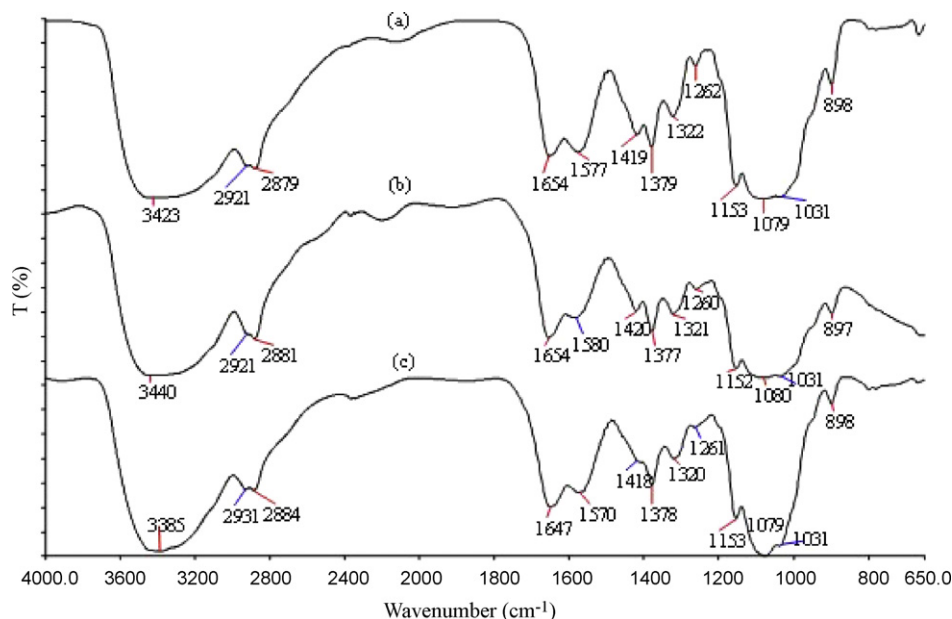


Fig. 2. FT-IR spectra of (a) unirradiated CS layer in the CS-glass system, (b) irradiated CS layer in the CS-glass system, (c) irradiated CS sub layer in the bilayer TiO₂-CS-glass system for 10 h in water.

carbonyl (C=O) side group. It was reported in the published literature, a strong absorption band of original CS ascribed to the $n \rightarrow \sigma^*$ transition for the amino groups, while the new absorption bands of irradiated CS ascribed to the $n \rightarrow \pi^*$ transition for the carbonyl and carboxyl side groups (Ulanski & Rosiak, 1992; Wang, Huang, & Wang, 2005).

3.3.2. Photoluminescence spectroscopy (PLS) spectral analysis

Fig. 4(a) and (b) shows the emission spectrum and fluorescent intensity of unirradiated CS layer in the CS-glass system and irradiated CS sub layer in the bilayer TiO₂-CS-glass system respectively performed at 325 nm excitation wavelength. As shown in Fig. 4(a), the typical emission spectra (λ_{em}) of unirradiated CS was observed at 500 nm (Kumar, Dutta, & Sen, 2010), at the excitation wavelength of 325 nm. On the other hand, the emission spectrum (b) shows significant reduction in the emission intensity and also red-shifted to around 525 nm. In this regard, Kumar et al. (2010) reported that the reduction of the emission intensity was due to the grafting of the electron-withdrawing groups in the CS backbone, while the red-shift was due to the richer electron content of CS structure by the attachment of the conjugates side group to the CS structure which would enlarge the degree of delocalized π -bond on the

whole molecular structure of CS. In fact, this explanation corresponds well with our presumption in this study about the formation of carbonyl (C=O) group as an electron-withdrawing side group in the structure of the photocatalytically oxidized CS. The presence of carbonyl group in the structure of the photocatalytically oxidized CS is considered to be responsible for the reduction in the emission intensity and caused the red-shift as well.

3.4. Surface studies

3.4.1. Surface morphology of CS

Fig. 5(a) and (b) shows representative SEM images of unirradiated and irradiated CS sub layer in the bilayer TiO₂-CS-glass system respectively for 10 h in water. In fact, the relatively smooth and regular surface of unirradiated CS sub layer had been converted into irregular, wavy surface with intense color, which is ascribed to the structural changes obtained by the forming of the

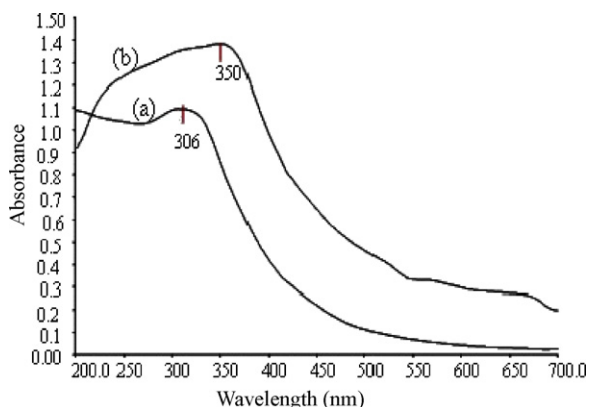


Fig. 3. UV-vis DRS spectra of (a) unirradiated CS layer in the CS-glass system and (b) irradiated CS sub layer in the bilayer TiO₂-CS-glass system for 10 h in water.

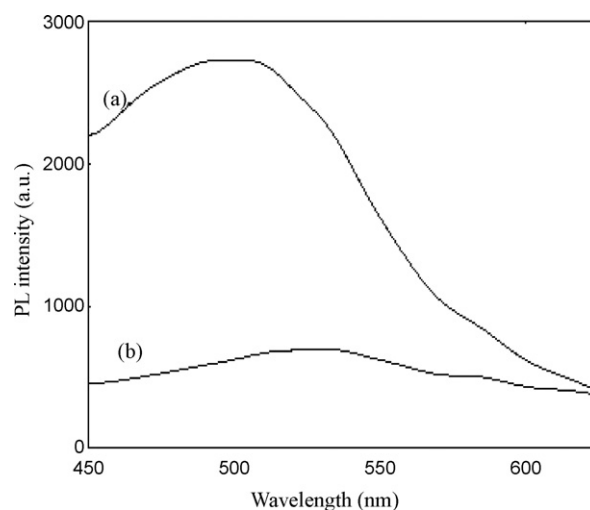


Fig. 4. Smoothed photoluminescence spectra of (a) unirradiated CS layer in the CS-glass system and (b) irradiated CS sub layer in the bilayer TiO₂-CS-glass system for 10 h in water, at excitation wavelength 325 nm.

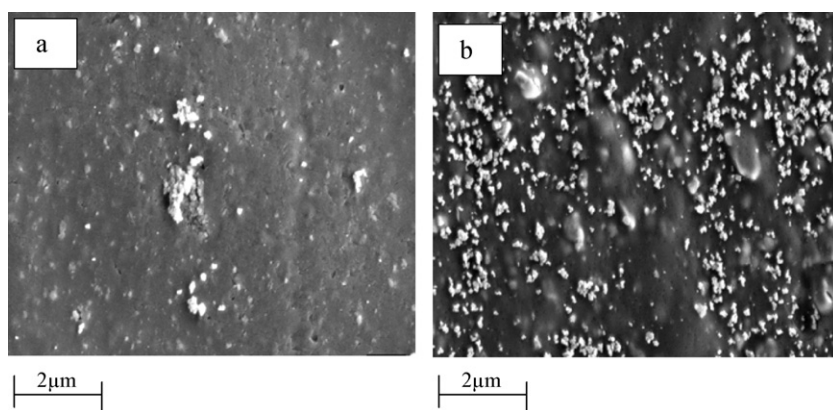


Fig. 5. SEM micrographs of CS sub layer in the bilayer TiO₂-CS-glass system (a) before and (b) after 10 h of irradiation in water, at 5000× magnification.

carbonyl side group in the photocatalytically oxidized CS structure. As for, the ultra fine white particles on both unirradiated and irradiated CS sub layer surfaces were ascribed to the ultra fine TiO₂ particles remained on the CS surface after the washing process.

3.4.2. Color change of CS

Fig. 6(a) and (b) shows the photographs of the visual color changes of unirradiated CS layer in the CS-glass system and irradiated CS sub layer in the bilayer TiO₂-CS-glass system respectively for 10 h in water. As can be seen, the color of irradiated CS sub layer obviously changed to a more intense brown, which is ascribed to the structural changes due to the formation of the carbonyl chromophore group in the chemical structure of the photocatalytically oxidized CS. The same observation was reported by other researchers when the CS was subjected to the different irradiation dose (Choi, Ahn, Lee, Byun, & Park, 2002), and different light sources (Felinto et al., 2007).

Furthermore, recently Zainol, Akil, and Mastor (2009) reported that the browning in color of irradiated CS solution by γ -irradiation is a fundamental function to the formation of carbonyl group.

3.5. Mechanistic discussion

It is well known that the TiO₂ is excited with light of wavelength $\lambda \leq 380$ nm (3.2 eV). Then, the electrons are promoted from the valence band (VB) to the conduction band (CB), generating positive holes and free electrons (Gaya & Abdullh, 2008), Eq. (3):



In an aqueous solution, the photolysis of water leads to the adsorption of hydroxyl ion on the catalyst surface in the dissociative form as (OH⁻ and H⁺), Eq. (4):



Hence, the positive hole reacts with a surface-bound hydroxyl ion, producing very powerful hydroxyl radicals ($\bullet\text{OH}$), Eq. (5).



The $\bullet\text{OH}$ radicals derived from an irradiated TiO₂ surface (Eq. (5)) migrated to the surface of the CS sub layer and can readily attacked any carbon atom in the pyranose ring of CS, since all the CH sites in the pyranose ring and also primary alcoholic ($-\text{CH}_2\text{OH}$) substitute group have the same selectivity towards the very active

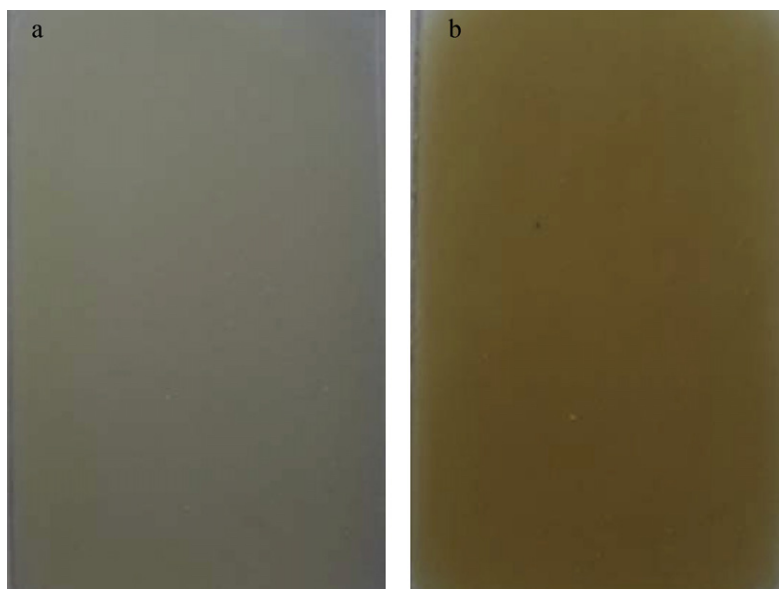


Fig. 6. The photographs of (a) unirradiated CS layer in the CS-glass system and (b) irradiated CS sub layer in the bilayer TiO₂-CS-glass system for 10 h after the complete removal of the TiO₂ top layer.

•OH radicals (Ulanski & von Sonntag, 2000). In fact, the generated hydroxyl radical by light-induced TiO_2 photocatalyst can readily abstract a proton from C-5, while the presence of oxygen (O_2) enable the formation of peroxy radical at the same C-5 position which eventually led to simultaneous removal of hydroxymethyl

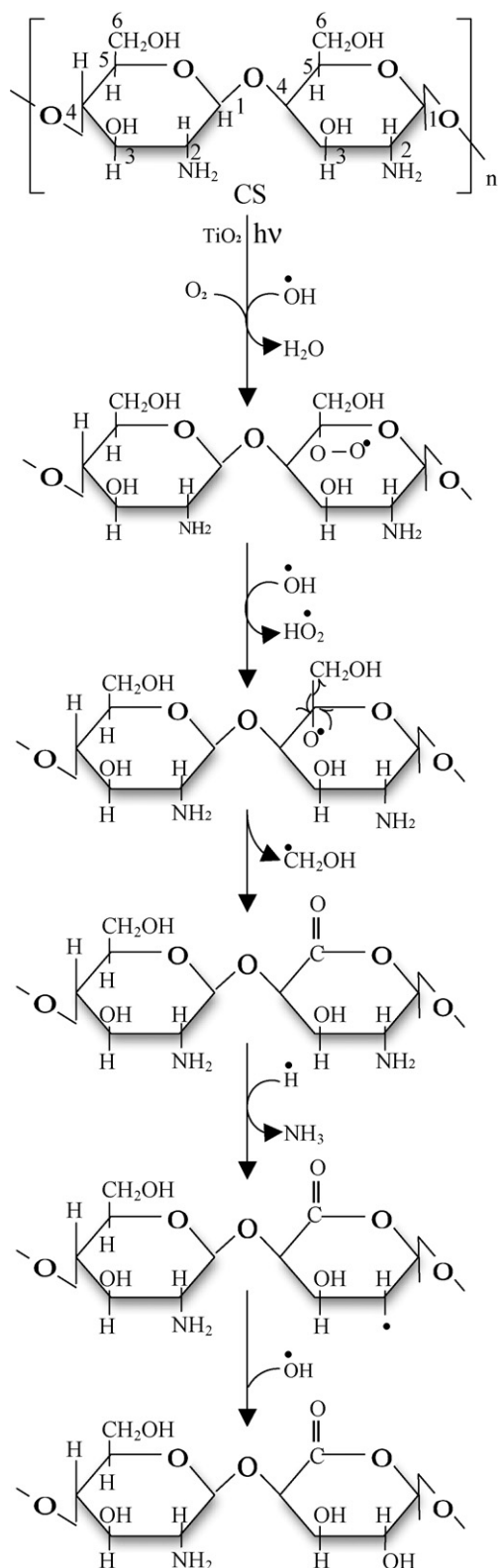


Fig. 7. Proposed structure of the photocatalytically oxidized CS sub layer in the bilayer TiO_2 -CS-glass system.

radical and the formation of the carbonyl group at C-5 position. In this regard, Sionkowska et al. (2005) reported that the photo-oxidation of the solid state CS film under UV light occurred by abstracting the primary alcoholic group ($-\text{CH}_2\text{OH}$) from C-5 of pyranose ring and forming the free radical. The role of oxygen was to form the peroxy radicals, after which the hydroxyl radical can easily undergo elimination resulting in the formation of the carbonyl side group at C-5. As for, the partial elimination of the amino group in the photocatalytic-oxidation process, it was reported that the photo-modification of solid state CS by γ -rays leads to the decay of amino groups without any further scission caused in the CS structure (Rosiak, Ulanski, Kucharska, Dutkiewicz, & Judkiewicz, 1992; Ulanski & Rosiak, 1992), while Huang et al. (2007) suggested that the partial elimination of amino group at C-2 of the carboxymethylated CS solution under γ -rays led to simultaneous formation of hydroxyl group at C-2. Thus, these mechanisms may explain the reduction in the percent nitrogen detected in the photocatalytically oxidized CS in this study and its apparent LR and SI as well. As mentioned, the experimental data described earlier in this study indicated that there was no major structural change of CS but a decrease in percent C and an appearance of carbonyl group with partial loss of amino groups. Therefore the most likely structure as the end product of the photocatalytic-oxidation process of CS in the solid state form and in the presence of TiO_2 under mild irradiation condition can be proposed and represented in Fig. 7.

4. Conclusion

By a simple bilayer assemblage of TiO_2 -CS-glass system, CS could be effectively oxidized under a low-energy 45-W compact household fluorescent lamp. The characterizations results indicated that the photocatalytic-oxidation of CS took place without altering much of the overall polymeric structure of CS. Furthermore, the CHN analyses and optical properties indicated clearly the lost of primary alcoholic group ($-\text{CH}_2\text{OH}$) with the formation of the carbonyl ($\text{C}=\text{O}$) side groups and partial elimination of amino groups. Additionally, the browning in CS color and the observable changes in the surface morphology of the photocatalytically oxidized CS were due to the modification of CS structure. In fact, this novel method of photocatalytic-oxidation process of CS can be considered as a convenient, potentially applicable and environmentally friendly.

Acknowledgements

The authors would like to thank the Ministry of Ministry of Science, Technology and Innovation (MOSTI) for supporting this project under Science Fund Grant: 305/pkimia/613402 and FRGS Grant (203/pkimia/671027). We would also like to acknowledge Universiti Sains Malaysia for the USM Fellowship for funding Ali H. Jawad and S. Sabar.

References

- Andrady, A. L., Torikai, Y., & Kobatake, T. (1996). Spectral sensitivity of chitosan photodegradation. *Journal of Applied Polymer Science*, 62, 1465–1471.
- Choi, W.-S., Ahn, K.-J., Lee, D.-W., Byun, M.-W., & Park, H.-J. (2002). Preparation of chitosan oligomers by irradiation. *Polymer Degradation and Stability*, 78, 533–538.
- Felinto, M. C. F., Parra, D. F., Silva, C. C., Angerami, J., Oliveira, M. J. A., & Lugão, A. B. (2007). The swelling behavior of chitosan hydrogels membranes obtained by UV- and γ -radiation. *Nuclear Instruments and Methods Physics Research B*, 265, 418–424.
- Gaya, U. I., & Abdullh, A. H. (2008). Heterogeneous photocatalytic degradation of organic contaminants over titanium dioxide: A review of fundamentals, progress and problems. *Journal of Photochemistry and Photobiology C: Photochemistry Reviews*, 9, 1–12.
- Gryczka, U., Dondi, D., Chmielewski, A. G., Migdal, W., Buttafava, A., & Fautitano, A. (2009). The mechanism of chitosan degradation by gamma and e-beam irradiation. *Radiation Physics and Chemistry*, 78, 543–548.

- Huang, L., Zhai, M., Peng, J., Li, J., & Wei, G. (2007). Radiation-induced degradation of carboxymethylated chitosan in aqueous solution. *Carbohydrate Polymers*, 67, 305–312.
- Kasaai, M. R., Arul, J., Chin, S. L., & Charlet, G. (1999). The use of intense femtosecond laser pulses for the fragmentation of chitosan. *Journal of Photochemistry and Photobiology A: Chemistry*, 120, 201–205.
- Kumar, S., Dutta, P. K., & Sen, P. (2010). Preparation and characterization of optical property of crosslinkable film of chitosan with 2-thiophenecarboxaldehyde. *Carbohydrate Polymers*, 80, 563–569.
- Liu, N., Chen, X. G., Park, H. J., Liu, C. G., Liu, C. S., Meng, X. H., et al. (2006). Effect of MW and concentration of chitosan on antibacterial activity of *Escherichia coli*. *Carbohydrate Polymers*, 64, 60–65.
- Nawi, M. A., Sabar, S., Jawad, A. H., & Ngah, W. S. W. (2010). Adsorption of reactive red 4 by immobilized chitosan on glass plates: Towards the design of immobilized TiO₂–chitosan synergistic photocatalyst-adsorption bilayer system. *Biochemical Engineering Journal*, 49, 317–325.
- Ngah, W. S. W., & Fatinathan, S. (2006). Chitosan flakes and chitosan–GLA beads for adsorption of *p*-nitrophenol in aqueous solution. *Colloids and Surfaces A: Physicochemical and Engineering Aspects*, 277, 214–222.
- Ostrowska-Czubenko, J., & Gierszewska-Drużyńska, M. (2009). Effect of ionic crosslinking on the water state in hydrogel chitosan membranes. *Carbohydrate Polymers*, 77, 590–598.
- Pawlak, A., & Mucha, M. (2003). Thermogravimetric and FTIR studies of chitosan blends. *Thermochimica Acta*, 396, 153–166.
- Peter, M. G. (2002). Chitin and chitosan from animal sources. In E. J. Vandamme, & S. De Baets (Eds.), *Biopolymers. Polysaccharides II. Polysaccharides from eukaryotes* (pp. 485–574). Weinheim: Wiley.
- Qin, C., Li, H., Xiao, Q., Liu, Y., Zhu, J., & Du, Y. (2006). Water-solubility of chitosan and its antimicrobial activity. *Carbohydrate Polymers*, 63, 367–374.
- Rosiak, J., Ulanski, P., Kucharska, M., Dutkiewicz, J., & Judkiewicz, L. (1992). Radiation sterilization of chitosan sealant for vascular prostheses. *Journal of Radioanalytical and Nuclear Chemistry*, 159, 87–96.
- Shao, J., Yang, Y., & Zhong, Q. (2003). Studies on preparation of oligoglucosamine by oxidative degradation under microwave irradiation. *Polymer Degradation and Stability*, 82, 395–398.
- Sionkowska, A., Wisniewski, M., Skopinska, J., Vicini, S., & Marsano, E. (2005). The influence of UV irradiation on the mechanical properties of chitosan/poly (vinyl pyrrolidone) blends. *Polymer Degradation and Stability*, 88, 261–267.
- Smitha, B., Sridhar, S., & Khan, A. A. (2005). Chitosan–sodium alginate polyion complexes as fuel cell membranes. *European Polymer Journal*, 41, 1859–1866.
- Ulanski, P., & Rosiak, J. (1992). Preliminary studies on radiation-induced changes in chitosan. *Radiation Physics and Chemistry*, 39, 53–57.
- Ulanski, P., & von Sonntag, C. (2000). OH-radical-induced chain scission of chitosan in the absence and presence of dioxygen. *Journal of Chemistry Society: Perkin Transactions*, 2, 2022–2028.
- Wan, Y., Creber, K. A. M., Peppley, B., & Bui, V. T. (2003). Ionic conductivity of chitosan membranes. *Polymer*, 44, 1057–1065.
- Wang, S.-M., Huang, Q.-Z., & Wang, Q.-S. (2005). Study on the synergetic degradation of chitosan with ultraviolet light and hydrogen peroxide. *Carbohydrate Research*, 340, 1143–1147.
- Zainol, I., Akil, H. M., & Mastor, A. (2009). Effect of γ -irradiation on the physical and chemical properties of chitosan powder. *Materials Science and Engineering C*, 29, 292–297.